EUROFUSION WPTFV-PR(15) 14262

C Day et al.

Effect of the dome on the collisional neutral gas flow in the DEMO divertor

Preprint of Paper to be submitted for publication in
IEEE Transactions on Plasma Science

This work has been carried out within the framework of the EUROfusion Consortium and has received funding from the Euratom research and training programme 2014-2018 under grant agreement No 633053. The views and opinions expressed herein do not necessarily reflect those of the European Commission.

Effect of the dome on the collisional neutral gas flow in the DEMO divertor

Chr. Day, S. Varoutis, Yu. Igitkhanov
Karlsruhe Institute of Technology (KIT),
Institute of Technical Physics, Vacuum Department
Karlsruhe, Germany
juri.igitkhanov@partner.kit.edu

***Abstract*—This paper presents analyses of the dome effect on the pumping efficiency and screening of the neutrals for the European DEMO ITER-like divertor configuration. The effect of the dome on neutral compression in the private flux region is assessed by using the DIVGAS code based on the Direct Simulation Monte Carlo method. The numerical analysis includes the calculation of neutral density, temperature and pressure in the divertor plenum and the overall conductance of the sub-divertor structure, which consequently affects the estimation of the effective pumping speed. It is shown that the divertor configuration with dome impedes the reflux of neutrals towards the plasma. In addition, due to the presence of intermolecular interactions, the dome does not strongly influence the macroscopic quantities near the pumping duct. A strong reflux of neutrals in the case without dome which was previously found in the free molecular flow regime is confirmed to be present also in the case of collisional flow.**

Keywords*—*DEMO; detachment; divertor; fueling; pumping efficiency; DSMC method.

I. INTRODUCTION

The design of the DEMO divertor cassette requires a new assessment of the role of the divertor dome structure under operational conditions. The primary function of the dome is to achieve a high compression of neutrals in the private flux region (PFR) in order to make the pumping efficiency and helium removal from the reactor more efficient. Additionally, the dome could reduce the neutral reflux to the core plasma through the x-point and shield the pump duct from neutrons. On the other side, it shadows the bottom surface of the divertor cassette from neutrons (which otherwise could be used for installation of a breeding blanket), is increasing the complexity of the divertor design and, eventually, the machine cost.

The above re-assessment requires the investigation of the neutral flow field in the whole range of gas rarefaction. For this task we will utilize a new and efficient numerical tool called DIVGAS, which is based on the Direct Simulation Monte Carlo (DSMC) method [1]. Just recently, it was used to model the neutral gas flow in the JET sub-divertor and a successful comparison with corresponding experimental results has been performed [2,3].. In this method, the solution of the Boltzmann kinetic equation is circumvented by simulating group of model particles that statistically mimic the behavior of real molecules for an arbitrary level of the gas rarefaction. The calculation of macroscopic parameters of practical interest is based on averaging the microscopic quantities in each grid cell of the flow field.

In the present work the DIVGAS code is applied for the case of D_2 gas flow through the DEMO sub-divertor structure with and without a dome. First results of a comparison between divertor operation with and without the dome have been performed for the ITER divertor and reported in [4]. The analysis showed the importance of the dome mainly due to the neutral gas compression, which is beneficial for helium exhaust [5].

The first assessments of the dome effect in DEMO design have been reported in the framework of a free molecular approximation (collisionless case) [6]. It was found that the DEMO dome structure can facilitate the pumping efficiency (about 2 times) and protect bulk plasma from reflux of neutral particles from the PFR. In the DEMO reactor, the major radius is 1.5 times larger than in ITER, therefore the size of the DEMO ITER-like divertor cassette and the divertor plenum is bigger than that in ITER. Also, the neutral density in the PFR could be high since the average bulk plasma density in DEMO is equal to or higher than that in ITER. This tendency has been observed in Alcator C-MOD experiments reported in [7]. Therefore, the dome effect on the DEMO divertor performance should be based on a nonlinear neutral transport treatment rather than a linear one. Thus, the aim of this work is to extend the aforementioned collisionless analysis by introducing the intermolecular interactions and in parallel to study their influence on the complete flow behaviour.

The overall numerical analysis done with the DIVGAS code includes the calculation of pressure, density and temperature fields as well as the gas flow pattern in the PFR and the sub-divertor area.

II. DEMO ITER-LIKE DIVERTOR GEOMETRY

The new baseline EU DEMO 2015 configuration with the aspect ratio 3.1 and 18 TF coils (R=8.8m, a=2.826 m, I_p=19.5 MA, plasma surface area S~1331 m^2) is considered in the present work [8]. The 3D geometrical configurations of the DEMO divertor with and without dome are shown in Fig.1.

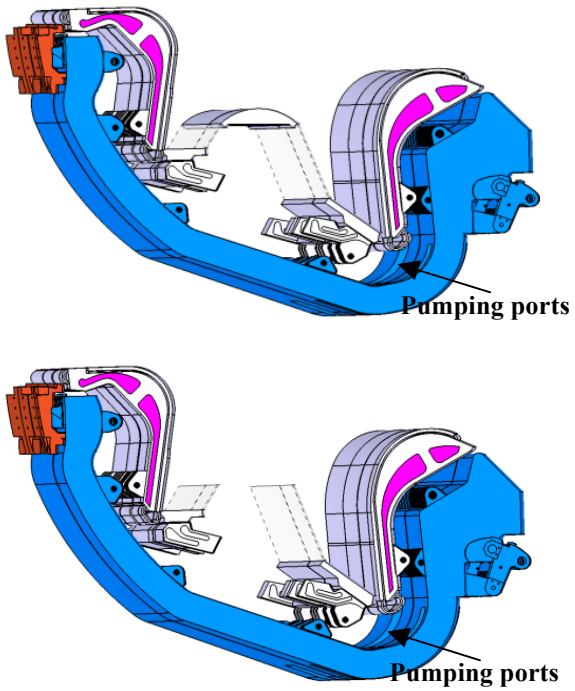

Fig.1. The 3D view of the two DEMO divertor cassettes with (top) and without (bottom) dome.

The PFR below the dome is separated from the plasma fan in the low field side (lfs) and high field side (hfs) by transparent side windows (Fig.1 dashed lines). The gaps between the cassette structure (shown in blue) and the vertical divertor plates and baffles provide a sink for neutrals from the divertor plenum. In this particular design, the corresponding lengths in the poloidal direction for the upper right and upper left gaps are 0.03 m and 0.02 m, respectively. The poloidal length of the dome structure is equal to 0.36 m (see in Fig. 2). The pumping surface is located on the right bottom side of each cassette and its length in the poloidal direction is l_{pump}=0.66 m. It is noted that the pumping ports are toroidally discontinuous and the width of each port is equal to Δ_{pump}=0.3 m. In order the total pumping surface to be estimated, the total number of cassettes (N~48) is multiplied by the surface of each pumping port and is estimated as A_{pump}=14.4 m^2. The neutrals from the outer and inner SOL region, penetrate into the PFR through the lfs and hfs gaps (see Fig. 2). The corresponding poloidal length of those gaps is 0.35 m and 0.13 m, respectively.

III. Boundary Conditions

The computational triangular grid used for the simulation of D_2 neutral particles in the plasma-free area as well as the corresponding boundary conditions on each surface, are shown in Fig. 2. The applied grid was chosen in general such that the cell size is smaller than the mean free path of D_2.

The boundary conditions which are assumed on the pumping surface are represented by a given capture coefficient ξ, which implies the probability of a neutral particle to be absorbed on this surface. Consequently, ξ varies between $0 \leq \xi \leq 1$. It is noted that ξ represents the imposed condition of fixed pumped particle flux and is related with the effective pumping speed $Seff$ of the pumping surface via the following equation

$$Seff = 14AvT\xi,$$

where vT is the thermal velocity and A the area of this surface. In reality, this pumping surface corresponds to the entrance of a duct having a density dependent conductance and connects the divertor structure with the pump [8]. As a result, the effective pumping speed and consequently the capture coefficient depend on the density of the duct as well. The discussion of how $Seff$ or ξ are related with the density is omitted in this paper, but it will be detailed analysed in future work. As a first approximation, a parametric analysis by varying the capture coefficient ξ is considered here. Additionally, it is assumed that the neutral gas temperature at the entrance to the pumping duct is equal to 420 K.

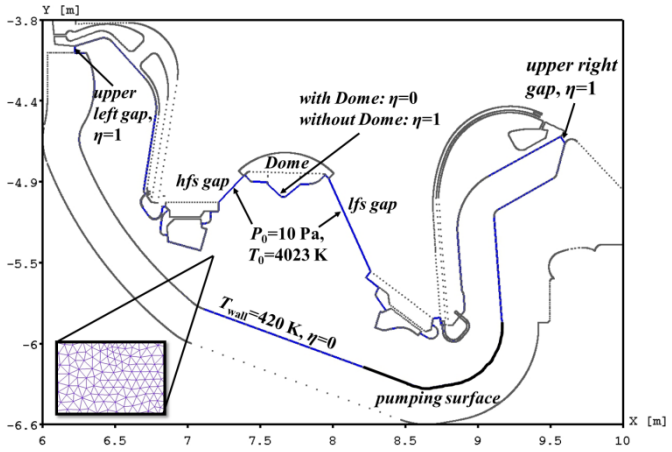

Fig.2. Geometrical configuration of the DEMO divertor, a uniform triangular mesh (shown in the zoomed area) and the corresponding boundary conditions are shown. The pumping surface is indicated at the right bottom side by a black solid line.

As far as the other than divertor boundaries are concerned we are specifying an absorption coefficient of neutral particles defined as $\eta = 1 - \Phi^-/\Phi^+$, where Φ^- is the neutral flux towards the surface and Φ^+ is the reflected one. The boundary conditions for the dome surface are specified as η=0 in the case of dome and η=1 without dome. The latter case corresponds to gas expansion into vacuum, which is fully justified assuming a cold detached plasma configuration. Furthermore, at the end of the side 'shoulders', neutrals escape into vacuum and therefore the imposed boundary condition there is equal to η=1. Moreover, it is assumed that the hot neutrals which arrive into the PFR through the lfs and hfs gaps have a reference temperature and pressure equal to T_0=4023 K and P_0 =10 Pa (similar to the ITER case [9]) respectively. For the rest of the PFR wall surfaces, it is assumed that the particles after hitting the wall with temperature T_{wall}=420 K are diffusively reflected backwards and consequently it is deduced that the absorption coefficient is equal to η=0.

IV. Gas Flow Pattern

The streamlines of collisional D_2 flow in the PFR and sub-divertor area are shown in Fig. 3 and Fig. 4 for the cases without and with dome, respectively. It is obvious that the

principal source for the neutral density in the divertor PFR and sub-divertor area is the flux of ions neutralized at the target vertical plates. For given temperature and pressure the neutral particle flux into the divertor from the low and high field side gaps (see Fig. 2) is calculated to be 9.8E+22 $m^{-1}s^{-1}$.

In the case without dome (Fig. 3), a strong gas outflow in the PFR towards the x-point is formed (i.e Reflux of neutral particles). That flow can cause a thermal MARFE instability at the x-point and potentially lead to disruption. It is seen that the flow pattern is completely changed in the case with dome, such that the dome protects against the gas outflow in the PFR under the x-point which is not shown in the figures. Calculations show that in the case of $\xi = 1$ without dome several vortexes are formed. At the low field side gap partially a neutral outflow to the SOL region is observed. The total number of molecules per second and per poloidal length entering the area from the low field side gap is 1.39E+23 $m^{-1}s^{-1}$ six times less, than the entering area from the high field side which is equal to 8.78E+23 $m^{-1}s^{-1}$. About 3.27E+23 $m^{-1}s^{-1}$ molecules of D_2 are escaping from the PFR at the top. The number of molecules which are pumped out is about 3.55E+23 $m^{-1}s^{-1}$. The leakage flows in the upper left and upper right gaps are 9.71E+22 $m^{-1}s^{-1}$ and 2.04E+20 $m^{-1}s^{-1}$, respectively (see Fig. 3).

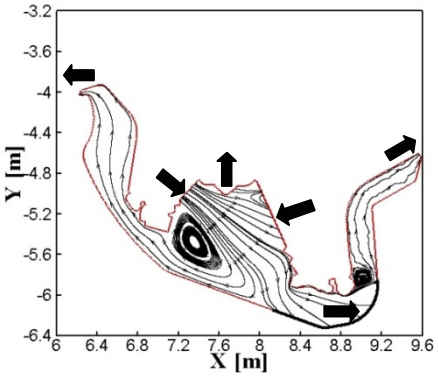

Fig.3. Streamlines of D_2 inside the plasma free area in the case without dome and ξ=1. A strong gas outflow is seen behind the x-point. Several vortexes are formed; the vortex in the low field side gap produces partially outflow of neutrals.

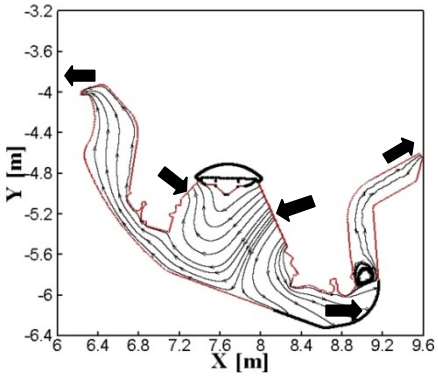

Fig.4. Streamlines of D_2 inside the plasma free area in the case with dome and ξ=1. it is seen that the dome protects the area behind the x-point from the gas outflow and no vortexes are formed.

In the case of the flow configuration with dome (Fig. 4) the reflux of neutrals behind the x-point is eliminated due to the presence of the dome structure. For this case, the number of molecules which are pumped is about 3.99E+23 $m^{-1}s^{-1}$, which is almost the same as in the case without dome and shows very moderate compression effect. The total number of molecules entering the PFR area from the lfs gap is 7.00E+23 $m^{-1}s^{-1}$ and from the hfs there is a sink of D_2 molecules towards the SOL with particle rate equal to 1.77E+23 $m^{-1}s^{-1}$. The leakages in the upper left and upper right gaps are 1.44E+23 and 3.24 E+20 $m^{-1}s^{-1}$, respectively (see Fig. 4). For both the above cases, the observed low particle rate from the upper right gap is believed to be an outcome of the vortex formation at the beginning of the right hand side shoulder, which limits the particles to move in the upward direction (see Fig. 3 and 4).

V. Effect of Capture Coefficient on Particle Flux

Dependence of the D_2 reflux on capture coefficient ξ for the cases without dome is presented in the Fig. 5.

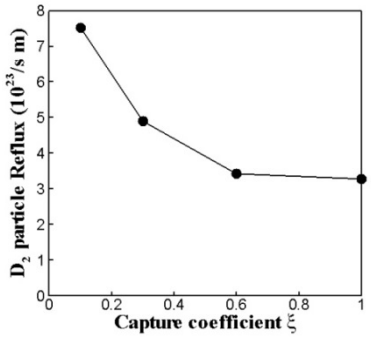

Fig.5. Reflux of D_2 molecules from the PFR to the plasma region in the case without dome versus the capture coefficient ξ.

It is shown that in the case without dome, the pumping efficiency is especially important in the regime of small capture coefficients. In other words, the reflux can be reduced about 2.3 times with increasing the pumping efficiency to values beyond ~ 0.4. In Fig. 6, it is depicted that, as expected, the pumped particle flux remains almost the same in the configuration with and without dome at any value of ξ. Actually, the main purpose of this figure is to quantify the pumped particle flux with respect to ξ and to cross-check the numerical outcome of the code since each point of the plot corresponds to an independent case study.

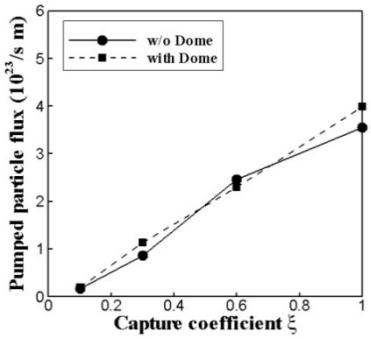

Fig.6. Pumped particle flux in configuration with and without dome for variable capture coefficient ξ.

VI. Molecular Gas Characteristics

The D_2 gas macroscopic quantities are calculated and presented below (Fig.7, 8 and 9) as contour plots of the density, temperature and pressure in the case without (top figure) and with dome (bottom figure), respectively. It is found that without the dome the plasma in the PFR boundary absorbs neutrals more efficiently so that density is lower in this area than with the dome. In Fig. 7, it is clearly illustrated the compression of neutral density below the dome area, whereas at the pumping surface the density in both cases is almost the same. Such effect justifies the necessity of the pumping location optimization. In Fig. 8, the effect of thermalization of particles, due to the presence of the dome, is shown. The neutral temperature in the case without dome is higher than in the dome case. This is because cold neutrals are reflected backwards after hitting the cold metallic dome structure. The contour plots of pressure are shown in Fig. 9. Since the density increase under the dome is compensated by D_2 temperature decrease, the difference in pressure is not so pronounced. We have found that this result is valid for any capture coefficient coefficient.

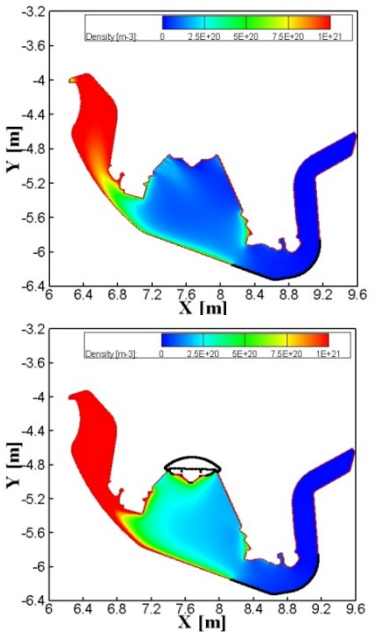

Fig.7. Density contour plot without (top) and with dome (bottom) and ξ=1. A density increase behind the dome region is clearly seen.

In the present work, it is suggested that the most representative parameter to characterize the operating point in the edge parameter space is the neutral pressure and density profile along the vertical line starting from the dome towards the bottom of the divertor and the line along the poloidal length of the pumping surface. In Fig. 10 and 11, the density distribution along this vertical line (see the sub-figure of Fig.10) and along the pumping surface (see the sub-figure of Fig.11) is shown, for the two considered configurations. As was mentioned above, the compression effect is also seen when comparing macroscopic quantities along the vertical line. The same conclusion is not valid for the quantities along the pumping duct, shown in Fig.11.

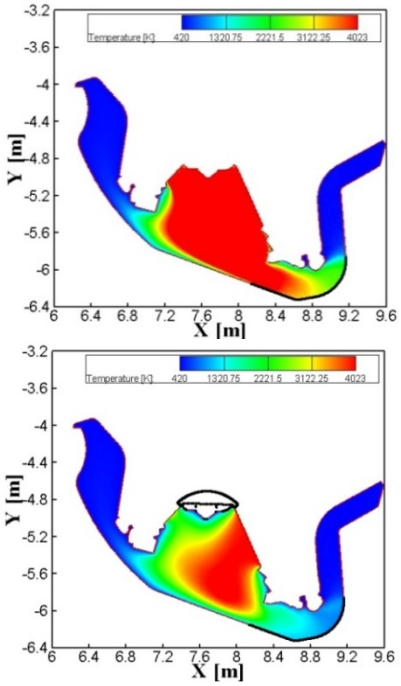

Fig.8. Temperature contour plot in the case without (top) and with dome (bottom) and ξ=1. In the former case hot area behind the x-point occurs due to hot molecules coming from the outer and inner divertor. In the latter case cooling of D_2 molecules occurs due to diffusive reflection of molecules with the dome bottom surface.

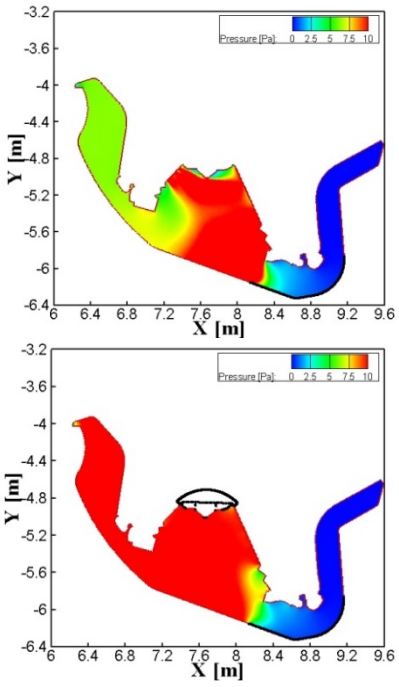

Fig.9. Pressure contours without (top) and with dome (bottom) and ξ=1. The results are not much different since the density increase is compensated by D_2 temperature drop.

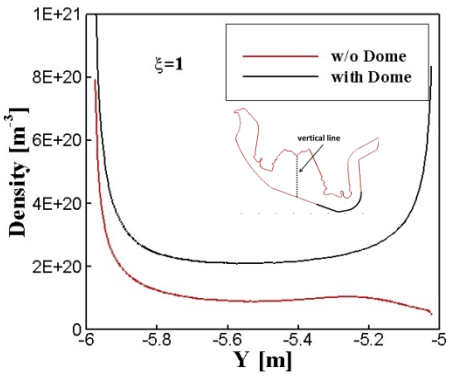

Fig.10. The density distribution along the vertical line for the cases with and without dome and ξ=1.

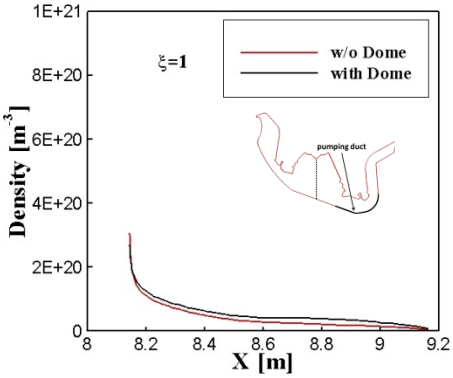

Fig.11. The density distribution along the pumping duct for the cases with and without dome and ξ=1.

VI. Conclusions

In this work we present preliminary results of the DIVGAS code calculation of the dome effect on the pumping efficiency and D_2 molecule characteristics in the DEMO ITER-like conventional divertor.

Calculations confirm that the divertor dome physically restricts the conductance between the PFR and the main chamber, enabling the density compression of the neutral gas. However the pressure change remains negligible due to the neutral cooling after interacting with the dome. Additionally, it is observed that the flow pattern is highly inhomogeneous in space and the dome has no direct influence on the macroscopic parameters at the pumping port. Therefore, it is unlikely to expect a noticeable facilitation of pumping efficiency and helium exhaust.

It is shown that without the dome, a strong reflux of the molecules towards the core and through the x-point and its vicinity can be expected. The neutrals have lower probability of reaching the pump duct since many of them return to the plasma in the area previously shielded by the dome. Therefore, the dome structure in the DEMO divertor can be favorable in protection of the x-point region on neutral influx with consequent possible thermal instability (MARFE) onset and, eventually, disruption occurrence. Moreover, in the case without the dome a strongly nonlinear flow streaming pattern occurs with vortexes forming neutral outflow from the PFR towards the SOL region. In the case of having the dome, calculations have shown that a strong outflux of neutrals from the high field side gap in the inner divertor is occurring. These neutrals can be reflected backwards undergoing only charge exchange in the SOL detached plasma. In the opposite case of an attached plasma in the SOL, it is expected that neutrals will be immediately ionized and eventually increase the recycling at the inner target plate. As a future work, the coupling of the DIVGAS code with a corresponding plasma code will be considered, in order to investigate the aforementioned predictions. Furthermore, it can be noted that a dome can protect the first wall surface from the hot neutrals and also to shield the pump duct from neutron irradiation.

On a longer time-scale, this work will be continued by considering multi-component plasma with different species like D_2, He, light impurities, ions and electrons. Electrons will be considered as independent species in order to take into account the residual plasma density in the PFR.

Acknowledgment

This work has been carried out within the framework of the EUROfusion Consortium and has received funding from the Euratom research and training programme 2014-2018 under grant agreement No 633053. The views and opinions expressed herein do not necessarily reflect those of the European Commission.

This work was supported by the Broader Approach Agreement between the European Atomic Energy Community and the Government of Japan, which provided resources for the Helios Supercomputer at IFERC-CSC under the Project DSMC_KIT.

References

[1] G. A. Bird, Molecular Gas Dynamics and the Direct Simulation of Gas Flows, Oxford University Press, Oxford, UK (1994).

[2] M. Groth, et al., “Impact of carbon and tungsten as divertor materials on the scrape-off layer conditions in JET”, Nucl. Fusion, **53**, (2013) 093016.

[3] S. Varoutis, et al., “Simulation of neutral gas flow in the JET sub-divertor and comparison with experimental results”, Proc. of the 25th IAEA Fusion Energy Conference (2014). To be published in Nuclear Fusion

[4] A. Kukushkin, H. Pacher, V. Kotov, et al., in Proceedings of the 32nd EPS, Tarragona (2005).

[5] H. Pacher, A. Kukushkin, G. Pacher, et al. J. Nucl. Mater., **313–316** (2003), pp. 657.

[6] Chr. Day, S. Varoutis , Yu. Igitkhanov, ‘Initial studies of the divertor dome effect on pumping efficiency in DEMO’, paper has been submitted in the Proceeding of the SOFE conference (2015).

[7] A. Niemczewski, et. al., Nuclear Fusion, **37** (2) (1997).

[8] V. Hauer, Chr. Day, Fus. Eng. Des. **84** (2009), pp. 903.

[9] V. Kotov, „Numerical study of the ITER divertor plasma with the B2-EIRENE code package“, Phd Thesis, FZ Jülich (2007).